Simulation-based optimum sensor selection design for an uncertain EMS system via Monte-Carlo technique

Simulation-based Optimum Sensor Selection Design for an Uncertain EMS System via Monte-Carlo Technique. ⋆

Konstantinos Michail *
Argyrios C. Zolotas, Roger M. Goodall **

* *Energy, Environment and Water Research Center, The Cyprus Institute, Nicosia, Cyprus (e-mail: kon_michael@ieee.org)*
** *Control Systems Group, Department of Electronic and Electrical Engineering, Loughborough University, Loughborough, UK (e-mail: {a.c.zolotas, r.m.goodall}@lboro.ac.uk)*

Abstract: Optimum sensor selection in control system design is often a non-trivial task to do. This paper presents a systematic design framework for selecting the sensors in an optimum manner that simultaneously satisfies complex system performance requirements such as optimum performance and robustness to structured uncertainties. The framework combines modern control design methods, Monte Carlo techniques and genetic algorithms. Without losing generality its efficacy is tested on an electromagnetic suspension system via appropriate realistic simulations.

Keywords: optimum sensor selection, modern control design, EMS systems, Monte Carlo, genetic algorithms

1. INTRODUCTION

Selecting the output measurements for controlling a system in an optimum manner is not a trivial task to do especially if many candidate sensor sets exist. The complexity, the often conflicting closed-loop objectives, the constraints and other control properties like optimum performance, robust performance and sensor fault tolerance make the problem even more complicated. Although the research community has considered the sensor selection before [Wal and Jager 2001] no systematic framework has been developed as flexible as the one presented in this paper able to handle many different conflicting closed-loop performance objectives subject to optimum sensor set selection. The novel sensor framework that is presented by the authors actually simplifies the sensor selection while ensuring the desired closed-loop response, optimum performance and robustness to structure uncertainties. The proposed sensor framework is very flexible and has been tested using various control strategies with many extensions developed by Michail [2009]. In this work, the framework is extended towards optimum sensor selection with robust performance and stability for an uncertain system. The key point of the approach is by incorporating **M**onte **C**arlo (MC) methods (see Roberto et al. [2004]) with the constraint handling techniques (that are used in **G**enetic **A**lgorithms (GA)). This idea has been roughly discussed before by the authors [Michail et al. 2008] but here a comprehensive description of the method is done along with appropriate simulations.

⋆ The Authors would like to thank Engineering and Physical Sciences Research Council, UK, for supporting this research work under the project Grand Ref. EP/D063965/1, and in part under the NEWACE project ref. EP/E055877/1, and BAE Systems from Systems Engineering Innovation Centre, UK.

The proposed systematic framework combines the $\mathcal{H}_\infty$ **L**oop **S**haping **D**esign **P**rocedure (LSDP) [McFarlane and Glover 1992], the GAs [Konak et al. 2006] and MC method for robustness assessment.
The **E**lectro-**M**agnetic **S**uspension (EMS) systems are being used on the **MAG**netic **LEV**itated trains [Lee et al. 2006]. As indicated by Goodall [2008] the EMS system is a non-linear, inherently unstable system with non-trial requirements and it can easily serve as a good example for testing the efficacy of the proposed framework.
This paper is separated into five sections: Section 2 describes the EMS model and the closed-loop requirements of the EMS. In Section 3 the details of the framework are given. Section 4 discusses the simulation results and the efficacy of the proposed framework is assessed. The paper concludes by summarizing the advantages in Section 5.

2. EMS MODELLING AND REQUIREMENTS

2.1 The EMS Model

The single degree-of-freedom model represents the quarter of a typical MAGLEV vehicle and is analysed here. As shown by Goodall [2004] a single-stage electro-magnetic suspension is suitable for low speed vehicles. The basic quarter car diagram of the MAGLEV vehicle is shown in Fig. 1. The suspension consists of an electromagnet with a ferromagnetic core and a coil of N_c turns which is attracted to the rail that is made of ferromagnetic material. The carriage mass (M_s) is attached on the electromagnet, with z_t the rail's position and z the electromagnet's position. The airgap $(z_t - z)$ is to be controlled so as to vary around the nominal operating condition. There are four important variables in an electromagnet named as force F,

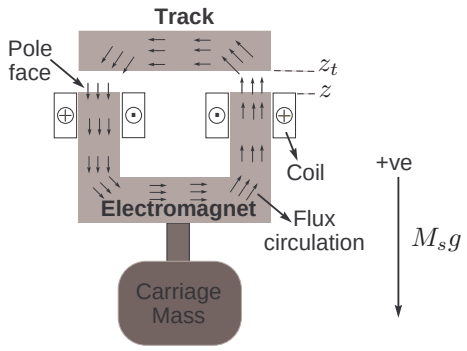

Fig. 1. Single-stage suspension for MAGLEV vehicles.

flux density B, airgap G and the coil's current I that give non-linear characteristics to the suspension as described in Goodall [2008]. Assuming that the motion vertically downwards is taken as positive the non-linear model of the EMS system is described by Newton's equation of motion in (1) and the voltage V_c in (2) across the electromagnet's coil from Kirchoff's law. Equations (3) and (4) give the force and flux density and the airgap velocity respectively [Goodall 2008].

$$M_s \frac{d^2 Z}{dt^2} = M_s g - F \tag{1}$$

$$V_c = I R_c + L_c \frac{dI}{dt} + N_c A_p \frac{dB}{dt} \tag{2}$$

$$B = K_b \frac{I}{G},\ F = K_f B^2 \tag{3}$$

$$\frac{dG}{dt} = \frac{dz_t}{dt} - \frac{dZ}{dt} \tag{4}$$

where g is the gravity acceleration constant which is $9.81 m/s^2$. The linearisation of the non-linear MAGLEV suspension model is based on small perturbations around the operating point. The following definitions are used with lower case letters defining the small variation around the operating point and subscript 'o' referring to the operating point.

$$B = B_o + b, F = F_o + f \tag{5}$$

$$I = I_o + i, G = G_o + (z_t - z) \tag{6}$$

$$V_c = V_o + u_c, Z = Z_o + z \tag{7}$$

Following the linearization procedure as given by Goodall [2008] the state space description of the EMS system can be expressed in state space form as in (8) where the selected states are $x = [i \quad \dot{z} \quad (z_t - z)]^T$ and the output equation corresponds to the following five measurements: i the coil's current, b the flux density, $(z_t - z)$ the airgap, $\dot{z}$ the vertical velocity and $\ddot{z}$ the vertical acceleration. The matrices $A, B_{u_c}, B_{\dot{z}_t}$ and C are given by (9)-(11).

$$\dot{x} = Ax + B_{u_c} u_c + B_{\dot{z}_t} \dot{z}_t \tag{8}$$
$$y = Cx$$

$$A = \begin{bmatrix} -\dfrac{R_c}{L_c + \frac{K_b N_c A_p}{G_o}} & -\dfrac{K_b N_c A_p I_o}{G_o^2 \left(L_c + \frac{K_b N_c A_p}{G_o}\right)} & 0 \\ -2K_f \dfrac{I_o}{M_s G_o^2} & 0 & 2K_f \dfrac{I_o^2}{M_s G_o^3} \\ 0 & -1 & 0 \end{bmatrix} \tag{9}$$

$$B_{u_c} = \begin{bmatrix} \dfrac{1}{L_c + \frac{K_b N_c A_p}{G_o}} \\ 0 \\ 0 \end{bmatrix}, B_{\dot{z}_t} = \begin{bmatrix} \dfrac{K_b N_c A_p I_o}{G_o^2 \left(L_c + \frac{K_b N_c A_p}{G_o}\right)} \\ 0 \\ 1 \end{bmatrix} \tag{10}$$

$$C = \begin{bmatrix} 1 & 0 & 0 \\ \dfrac{K_b}{G_o} & 0 & -\dfrac{K_b I_o}{G_o^2} \\ 0 & 0 & 1 \\ 0 & 1 & 0 \\ -2K_f \dfrac{I_o}{M_s G_o^2} & 0 & 2K_f \dfrac{I_o^2}{M_s G_o^3} \end{bmatrix} \tag{11}$$

The output matric, C gives the five measurements (i.e. i,b,$(z_t - z)$,$\dot{z}$ and $\ddot{z}$) and the sensor sets can be obtained by using the corresponding rows of C in (11). The total number of sensor sets is $N_s = 2^{n_s} - 1$, where n_s is the total number of sensors. Given that the EMS system has 5 outputs there are 31 candidate sensor sets. However, since the LSDP controller design technique is used here and therefore the airgap measurement is a standard measurement, the number of candidate sensor sets reduces to 15. The electromagnet design of MAGLEV vehicles is described in more details by Goodall [Sep 1985]. A typical quarter car vehicle of $1000kg$ requires an operating force of $F_o = M_s \times g$. The operating airgap (G_o) is at $15mm$ to accommodate the track roughness. According to these requirements the rest of the parameters can be calculated and they are listed on Table 1.
The EMS system is inherently unstable system and is also characterised by uncertainties that can be caused from various reasons. Table 1 tabulates the uncertainties that could possibly occur.

Table 1. Parameters of the EMS system.

Par.	Val.	Unc.	Par.	Val.	Unc.
G_o	0.015m	10%	M_s	$1000kg$	10%
B_o	1T	10%	R_c	10Ω	50%
I_o	10A	10%	L_c	0.1H	50%
V_o	100V	0%	N_c	2000	0%
F_o	9810N	10%	A_p	$0.01m^2$	0%

Note: Par. - Parameter, Val. - Value, Unc. - Uncertainty

2.2 Design Requirements and Inputs to the EMS

Stochastic Inputs The stochastic inputs are random variations of the rail position as the vehicle moves along the track. This is caused by the steel rail installation discrepancies due to track-laying inaccuracies and unevenness. Considering the vertical direction, the velocity variations can be approximated by a double-sided power spectrum density (PSD) expressed as

$$S_{\dot{z}_t} = \pi A_r V_v \tag{12}$$

where V_v is the vehicle speed (taken as $15m/s$ in this case) and A_r represents the roughness which is assigned a value as $1 \times 10^{-7} m$ corresponding to high quality track. Then the corresponding autocorrelation function is given as:

$$R(\tau) = 2\pi^2 A_r V_v \delta(\tau) \tag{13}$$

Although a linear controller is used, the simulations are actually based on the implementation to the nonlinear model. Hence, we calculate the RMS values of the required

quantities (acceleration, current etc) using time history data.

Deterministic Input The main deterministic input to the suspension in the vertical direction is due to the transition onto a gradient. In this work, the deterministic input (see Fig. 2) is a gradient of 5% at a vehicle speed of $15m/s$, an acceleration of $0.5m/s^2$ and a jerk of $1m/s^3$.

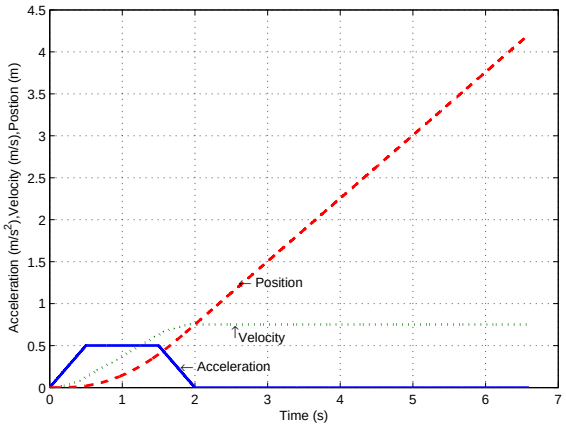

Fig. 2. Deterministic input to the suspension with a vehicle speed of $15ms^{-1}$ and 5% gradient.

EMS Control Properties The design requirements for an EMS system depend on the type and speed of the train. and they are well described in Goodall [1994, 2004]. His work is focused upon the low speed Birmingham Airport Maglev vehicle EMS suspension requirements which operated successfully in the UK for a period of 12 years in the 1980s and 1990s. Fundamentally, there is a trade-off between the deterministic and stochastic responses of the EMS system. Table 2 tabulates the design limitations for the deterministic and stochastic features. The deterministic features are limited to the maximum standard values and the stochastic ones are set as objectives to be minimized i.e. the vertical acceleration $\ddot{z}_{rms}$ (improve ride quality) and the RMS current variations i_{rms} from the stochastic response.
The robust stability margin (degree of robustness) ϵ calculated from the LSDP is maximized for maximum robustness to uncertainties (note that $\gamma = 1/\epsilon$).
Since noise affects the sensors, an amount of this noise will appear on the control effort $u_{n_{rms}}$ [Michail et al. 2009]. In that case the noise, if not eliminated, can be amplified from the controller hence its been set as an objective to be minimised.
Summarizing, the objective functions ϕ_i to be minimized are formally written as:

$$\phi_1 = i_{rms},\ \phi_2 = \gamma,\ \phi_3 = \ddot{z}_{rms},\ \phi_4 = u_{n_{rms}} \qquad (14)$$

3. THE SENSOR OPTIMISATION FRAMEWORK

The proposed framework can be summarised in the flow chart of Fig. 3. The particular points include the use of $\mathcal{H}_\infty$ loop-shaping design and the heuristic optimisation (evolutionary algorithms) method for tuning the controller subject to strict requirements (objectives and constraints)

Table 2. Constraints on the EMS system performance.

EMS limitations	Value
RMS acceleration,$\ddot{z}_{rms}$	$\leq 1ms^{-2}$
RMS airgap variation,$(z_t - z)_{rms}$	$\leq 5mm$
RMS control effort,$u_{c_{rms}}$	$\leq 300V(3I_0R_c)$
Maximum airgap deviation,$(z_t - z)_p$	$\leq 7.5mm$
Control effort,u_{c_p}	$\leq 300V(3I_0R_c)$
Settling time, t_s	$\leq 3s$
Airgap Steady state error,$(z_t - z)_{e_{ss}}$	$= 0$
Robust Stability Margin, ϵ	≥ 0.15

for each feasible sensor set of the EMS system.
Prior to running the algorithm (initialization phase), some parameters are assigned including evolutionary algorithms parameters, controller selection criteria (f_{c_i}) and the user's controller selection criterion (f_k). f_{c_i} and f_k make sure that the selected controller results in a desired closed-loop performance. Starting the optimisation procedure, the first sensor set is selected and the evolutionary algorithm seeks the Pareto-optimality of the objective functions in (14) (i.e. the trade-off between them) subject to the constraints listed on Table 2.
In the sequence, the algorithm seeks to find the optimized controller by using the overall constraint violation function,Ω (see (17) in Section 3.2). At this point there are two paths to follow:
(i) If there is no sufficient controller (this can be easily verified by checking Ω for each individual response) then the controller which gives the minimum Ω is selected and saved.
(ii) Those controllers satisfying Ω are selected. The next

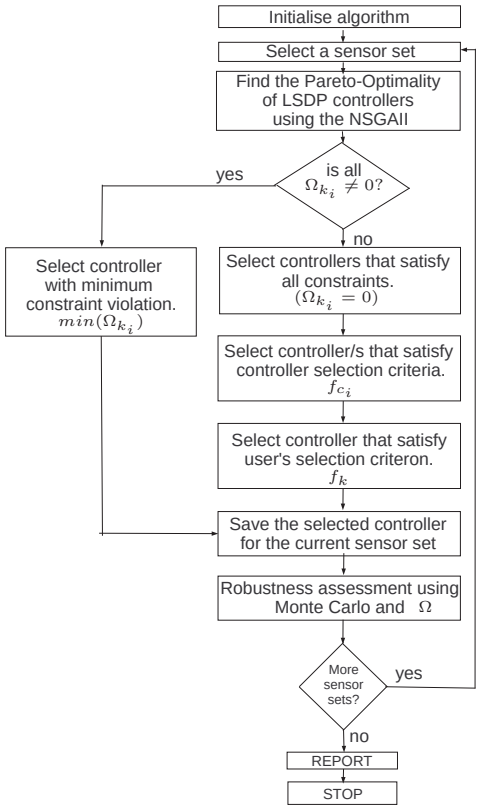

Fig. 3. Flow chart of the proposed sensor optimisation framework with robust $\mathcal{H}_\infty$ loop-shaping design.

step is to select those controllers that satisfy the controller selection criteria f_{c_i} and finally, the user's controller selection criteria, f_k is used to select the controller which results in the desired closed-loop response. If no controller exists to satisfy f_{c_i} then the algorithm directly selects a controller based only on f_k. The optimally tuned controller is saved and the algorithm moves to the next stage where robustness is assessed via MC method.
The particular sensor set and the selected controller provide a nominal performance that is assessed for parametric uncertainties by combining the MC method with the overall constraint violation function in the following way:
(i) For every q^{th} of the uncertain EMS system do: calculate the overall constraint violation function (Ω) using simulation results from the closed-loop response of the deterministic and stochastic profiles of the track.
(ii) From the closed-loop responses of the Q samples select the one with the maximum value of the overall constraint violation function. This is taken as the worse case overall constraint violation function noted as (Ω_{w-c}). In case the closed-loop response with an uncertain model is unstable, Ω_{w-c} is quantified by infinity.
In this way the robustness of the optimally tuned nominal controller is assessed. Finally, the algorithm moves to the next feasible sensor set until all feasible sensor sets are checked as described above.

3.1 $\mathcal{H}_\infty$ loop-shaping design

The design of the optimised controller is based on the normalised coprime-factor plant description, proposed by McFarlane and Glover [1992], which incorporates the simple performance/robustness tradeoff obtained in loop shaping, with the normalised left coprime factorization robust stabilization method as a means of guaranteeing closed-loop stability.
The design method proceeds by shaping the open-loop characteristics of the plant by means of the weighting functions $W1$ and $W2$ (see Fig. 4(a)). The plant is temporarily redefined as $\hat{G}(s) = W2GW1$ and the $\mathcal{H}_\infty$ optimal controller $\hat{K}(s)$ is calculated. In the final stage, the weighting functions are merged with the controller by defining the overall controller K(s)=$W1\hat{K}W2$ as shown in Fig. 4(b). The size of model uncertainty is quantified

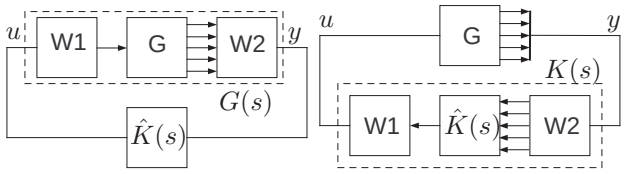

(a) *Shaped plant.* **(b) *Final controller.***

Fig. 4. H_∞ loop-shaping design.

by the stability radius ϵ (refer to McFarlane and Glover [1992] and Skogestad and Postlethwaite [2005] for more details), i.e. the stability margin. For values of $\epsilon \geq 0.25$, 25% coprime factor uncertainty is allowable. However, in this paper the coprime factor uncertainty is set to 15% i.e. $\epsilon \geq 0.15$.
In typical design the filter functions and thus the controller are to be kept as simple as possible. Thus, the $W1$ precompensator, is chosen as a single scalar weighting function set to unity. For the $W2$ post-compensators there can be five weighting functions that are used depending on the selected sensor set. The airgap $(z_t - z)$ measurement is a compulsory measurement required for proper maglev control of the magnet distance from the rail and thus a low pass filter ($W_{(z_t-z)}$) is chosen with integral action allowing zero steady state airgap error (for the nominal performance). The weighting functions are given as

$$W1 = 1; \quad W2 = diag(W_i, W_b, W_{(z_t-z)}, W_{\dot{z}}, W_{\ddot{z}}) \tag{15}$$

with,

$$W_{(z_t-z)} = \left(\frac{\frac{s}{M_p^{1/n_p}} + \omega_b}{s + \omega_b A_p^{1/n_p}} \right)^{n_p} \tag{16}$$

The above results in a minimum phase and stable weighting filter with roll-off rate n_p. Note that there exist 2^4 candidate sensor sets and that the airgap sensor is always required.

3.2 Multi-objective Constrained Optimisation

Heuristic approaches are very powerful optimisation tools which are used in many engineering problems. Particularly the GAs have been extensively implemented in control engineering (see Fleming and Purshouse [2002]). Different types of GAs have been developed in recent years and they are well summarized by Konak et al. [2006]. In this research work, the recently developed GA based on non-dominated sorting of the population, **N**on-dominated **S**orting **G**enetic **A**lgorithm II (NSGA-II) is used that proves to be a powerful optimization tool. For the interested reader details on NSGA-II are described by Deb et al. [2002]. NSGA-II is an evolutionary process that requires some parameters to be assigned in order to ensure proper population convergence towards Pareto-optimality. These are mainly selected from experience rather than from a-priori knowledge of the optimisation problem. The crossover probability is generally selected to be large in order to have a good mix of genetic material. The crossover probability is set to 90% and the mutation probability is defined as $1/n_u$ where, n_u is the number of variables. The population consists of 50 chromosomes and the stopping criterion is the maximum generation number N_{gen}. N_{gen} has a significant role on the Pareto-Optimality and the computational time i.e. the higher the generation number is the longer the computational time but it is more possible for the evolved population to converge and finally spread onto the optimum Pareto front. N_{gen} depends among other factors on the number of variables to be tuned because the larger the number of variables is a larger N_{gen} is required with the expense of having longer computational time. In this problem because the number of variables varies according to the number of sensors, N_{gen} is set at 200 for sensor sets with up to 3 sensors and for the rest including the full sensor set is set at 250 generations.
In order to achieve the desired closed-loop response a constraint handling technique is necessary. Constraint handling methods with genetic algorithms can be done differently as Coello [2002] indicates. The dynamically updated penalty function approach is used here to achieve the control constraints. A rigorous description of this method for the proposed systematic framework is described by

Michail [2009]. This method is using a function in order to 'guide' the objective functions in (14) towards the Pareto-optimality while the desired constraints on Table 2 are satisfied. The overall constraint violation function is given as

$$\Omega(k^{(j)}, f^{(i)}) = \sum_{j=1}^{J} \omega_j(k^{(j)}) + \sum_{i=1}^{I} \psi_i(f^{(i)}) \qquad (17)$$

where, ω_j is the j^{th} soft constraint violation for the corresponding j^{th} quantity to be constrained (k) and J is the total number of soft constraints. Similarly, ψ is the hard constraint violation for the i^{th} quantity to be constrained (f). The overall constraint violation function serves as a controller selection criterion within the systematic framework as described at the beginning of this section.

3.3 Robustness assessment within the framework

Taking advantage of the fact that any changes in the closed-loop response (both stability and performance) will be reflected on Ω in (17), robustness against parametric uncertainties can be tested in combination with MC technique. MC technique has been used in a variety of disciplines for many years now therefore the details are omitted. Monte Carlo is a probabilistic method that can be used to randomly sample the uncertain parameters of the EMS system and them to test the closed-loop stability and performance. This can be achieved by using a number of samples, Q of the uncertain EMS and test them using the nominal controller. In this paper 100 samples ($Q = 100$) of the EMS model are tested for each sensor set. Then, the worse-case value of Ω is taken that represents the worse-case response noted as Ω_{w-c}.

4. SIMULATIONS AND DATA ANALYSIS

The framework is tested in MATLAB R2009b simulation environment without Java function due to large computational need (simulation based). The computer used is the powerful DELL T610 with 2.93GHz Intel®Xeon®X5570 processor and 8GB RAM.The average simulation time per sensor set is about 2.5 hours while completion of the framework takes around 45 hours.

The controller selection criteria (f_{c_i}, f_k) for the desired closed-loop response are given as follows

$$f_{c_1} \equiv \ddot{z}_{rms} \leq 0.5m/s^2, f_{c_2} \equiv u_{n_{rms}} \leq 10V, \qquad (18)$$

$$f_k \equiv max(\epsilon) \qquad (19)$$

Recall that if f_{c_i} criteria are not satisfied then the best controller selection is done based only on f_k. The first set of closed-loop desired characteristics in (18) ensures that the controllers to be selected are within the limits indicated while the last criterion in (19) ensures that the selected controller has the maximum robust stability margin (maximum robustness).

From the results it was found that the proposed systematic framework is able to identify stabilizing controllers that satisfy (17),(18) and (19) for 11 out of 16 sensor sets. The other four violate (17) hence the performance is not satisfactory. However, they could be used if the constraint violation does not threaten the safety of the system.

Table 3 lists some sensor sets that are selected for comprehensive analysis of the results. The second column lists the sensor sets and the first the corresponding identification number. The next four columns are the variables from the closed-loop response with the stochastic track profile and the further four show the variable values from the deterministic profile. The next column is the resulting stability margin from the $\mathcal{H}_\infty$ loop-shaping design and the 12^{th} column lists the resulting RMS level of the noise on the input voltage. The 13^{th} column shows whether the overall constraint violation function, Ω is satisfied or not (without any uncertainties i.e. the nominal closed-loop response). The last column represents the worse-case overall violation function, Ω_{w-c}. That is the maximum value of Ω among the resulted closed-loop responses using the Q samples of the uncertain EMS system. If the worst-case response is instability of the closed-loop then the Ω_{wc} is assigned to be infinity.

Inspecting the Ω column that reflects the nominal performance of the EMS system it can be seen that id:1 and 2 violate the stability margin while the rest of the sensor sets satisfy it. Comparing the EMS performance with id:8 (i.e. the full sensor set) and the rest of the sensor sets is observed that similar nominal response can be achieved with fewer sensors eg. id:3. However, when the performance against parametric variations is assessed with Monte Carlo it becomes difficult to achieve robustness while in some cases the worst case is instability eg. id:1. The sensor set id:1 has a value of infinity Ω_{w-c} which means that there is a combination of uncertain EMS parameters that cause instability. The best robust performance is achieved with id:7 comprising of 4 sensors and it gives a Ω_{w-c} of 1.21 that means for a particular combination of the uncertain parameters there is some control constraint violation. Nevertheless, this is the best sensor set with which robust performance of the EMS system can be achieved. Figure 5 depicts the Pareto-Optimality with id:7 (note that the values are normilized around one for good resolution). It is clear that the trade-off between the objective functions is successfully found. Figure 6 illustrates the airgap deflections of the closed-loop response with the nominal controller and the deterministic input (the transition onto the track's gradient) by sampling 100 uncertain non-linear models of the suspension. The response of the suspension is restricted to the requirements as listed in Table 2. Although the steady state error is not zero is still very small and does not impose any serious danger for the operation of the suspension.

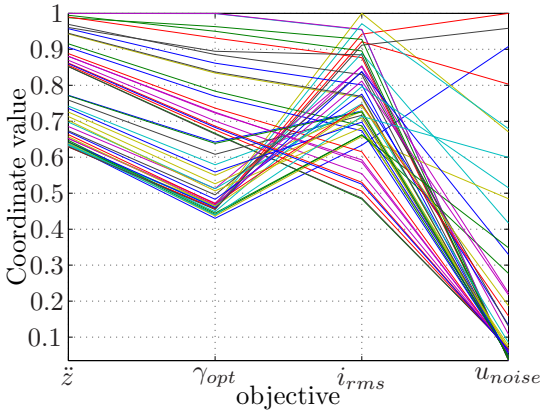

Fig. 5. Trade-off of the objective functions using id:6.

Table 3. Optimised sensor configurations for the EMS system.

		Stochastic input profile				Deterministic input profile							
		g_{rms}	$u_{c_{rms}}$	$\ddot{z}_{rms}$	i_{rms}	g_p	u_{c_p}	t_s	e_{ss}	ϵ	$u_{n_{rms}}$	Ω	Ω_{w-c}
id	Sensor set	mm	V	ms^{-2}	A	mm	V	s			V		
1	$(z_t - z)$	1.82	48.61	1.00	1.69	1.31	12.41	2.29	✓	**0.14**	0.26	x	∞
2	$b(z_t - z)$	1.82	48.79	1.00	1.69	1.32	12.44	2.29	✓	**0.14**	0.26	x	145
3	$(z_t - z)\ddot{z}$	1.85	43.42	0.96	1.68	2.32	18.87	2.19	✓	0.15	0.17	✓	23.34
4	$i(z_t - z)\ddot{z}$	1.68	45.40	0.99	1.68	2.19	18.07	2.18	✓	0.15	0.17	✓	38.80
5	$(z_t - z)\dot{z}\ddot{z}$	1.66	22.41	0.47	1.66	4.22	32.63	2.73	✓	0.15	0.47	✓	27.77
6	$ib(z_t - z)\ddot{z}$	*1.39*	*19.65*	*0.39*	*1.39*	*7.47*	*53.59*	*2.16*	✓	*0.15*	*0.45*	✓	*1.21*
7	$i(z_t - z)\dot{z}\ddot{z}$	1.83	45.81	0.99	1.68	2.08	17.35	2.19	✓	0.15	0.17	✓	67044
8	$ib(z_t - z)\dot{z}\ddot{z}$	2.13	23.05	0.49	1.64	3.59	27.69	2.68	✓	0.15	0.45	✓	24.59

$g_p \equiv (z_t - z)_p$,$g_{rms} \equiv (z_t - z)_{rms}$,$e_{ss} \equiv (z_t - z)_{e_{ss}}$

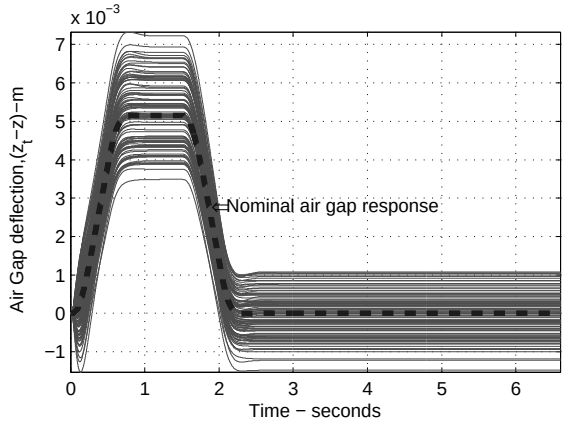

Fig. 6. Airgap deflections with 100 samples of the uncertain EMS using the sensor set with id:6.

5. CONCLUSION

This paper has shown that the proposed framework is able to identify the best sensor set with which the control of EMS system is possible subject to multiple and complex requirements that otherwise would be very difficult to achieve by manual design of the control system. It has been showed that with id:7 it is possible to control a complex electromechanical system like the EMS with non-linearities, uncertainties and multiple constrained control objectives. The framework is very flexible and without losing generality it can be easily adapted to many sensor selection problems in control systems provided that the dynamic model is well known.

REFERENCES

Coello, C.A.C. (2002). Theoretical and numerical constraint-handling techniques used with evolutionary algorithms: A survey of the state of the art. *Computer Methods in Applied Mechanics and Engineering*, 191(11-12), 1245–1287.

Deb, K., Pratap, A., Agarwal, S., and Meyarivan, T. (2002). A fast and elitist multiobjective genetic algorithm: Nsga-ii. *IEEE Transactions on Evolutionary Computation*, 6(2), 182–197.

Fleming, P.J. and Purshouse, R.C. (2002). Evolutionary algorithms in control systems engineering: A survey. *Control Engineering Practice*, 10(11), 1223–1241.

Goodall, R.M. (1994). Dynamic characteristics in the design of maglev suspensions. *Proceedings of the Institution of Mechanical Engineers, Part F: Journal of Rail and Rapid Transit*, 208(1), 33–41.

Goodall, R.M. (2004). Dynamics and control requirements for ems maglev suspensions. In *Proceedings on international conference on Maglev*, 926–934.

Goodall, R.M. (2008). Generalised design models for ems maglev. In *Proceedings of MAGLEV 2008 - The* 20^{th} *International Conference on Magnetically Levitated Systems and Linear Drives*.

Goodall, R.M. (Sep 1985). The theory of electromagnetic levitation. *Physics in Technology*, 16(5), 207–213.

Konak, A., Coit, D.W., and Smith, A.E. (2006). Multi-objective optimization using genetic algorithms: A tutorial. *Reliability Engineering and System Safety*, 91(9), 992–1007.

Lee, H.W., Kim, K.C., and Lee, J. (2006). Review of maglev train technologies. *IEEE Transactions on Magnetics*, 42(7), 1917–1925.

McFarlane, D.C. and Glover, K. (1992). A loop-shaping design procedure using h_∞ synthesis. *IEEE Transactions on Automatic Control*, 37(6), 759–769.

Michail, K. (2009). Optimised configuration of sensing elements for control and fault tolerance applied to an electro-magnetic suspension system. PhD dissertation, Loughborough University, Department of Electronic and Electrical Engineering. http://hdl.handle.net/2134/5806.

Michail, K., Zolotas, A.C., and Goodall, R.M. (2009). Ems systems: Optimised sensor configurations for control and sensor fault tolerance. *Japan Society of Mechanical Engineers, International Symposium on Speed-up, Safety and Service Technology for Railway and Maglev Systems*.

Michail, K., Zolotas, A.C., Goodall, R.M., and Pearson, J.T. (2008). Maglev suspensions - a sensor optimisation framework. In 16^{th} *Mediterranean Conference on Control and Automation*, 1514–1519.

Roberto, T., Giuseppe, C., and Fabrizio, D. (2004). *Randomized Algorithms for Analysis and Control of Uncertain Systems*. Springer.

Skogestad, S. and Postlethwaite, I. (2005). *Multivariable Feedback Control Analysis and Design*. John Wiley & Sons Ltd, 2^{nd} Edition, New York.

Wal, M.V.D. and Jager, B.D. (2001). A review of methods for input/output selection. *Automatica*, 37(4), 487–510.